Available online at www.sciencedirect.com
SCIENCE DIRECT®
Journal of Sound and Vibration 277 (2004) 419–428
JOURNAL OF SOUND AND VIBRATION
www.elsevier.com/locate/jsvi

Letter to the Editor

Active mass damping of electronic circuit boards

B. Esser*, D. Huston

Department of Mechanical Engineering, 201 Votey Building, The University of Vermont, Burlington, VT 05405-0156, USA

Received 10 November 2003; accepted 21 November 2003

1. Introduction

Aerospace electronics are subject to extremely harsh vibratory environments throughout their service lives. To ensure that critical electronic systems do not fail, they are mounted in bulky, heavy, and stiff fixtures which prevent damage to the electronic circuit boards (ECBs). The boards are also much thicker than traditional boards for static environments (such as PC boards) to provide needed stiffness, however these stiffened boards are also very heavy. It is proposed to actively damp these ECBs so as to keep the vibrations down to safe levels at a reduced weight and cost when compared to present passive vibration damping systems.

ECBs used in spacecraft, aircraft, and missile systems are exposed to severe shock and vibrations. Vibration frequencies seen in such systems can range from 3 to 5000 Hz, with acceleration levels from 1 to 30 G [1]. Much effort has gone into producing systems capable of surviving this environment, however these efforts also greatly increase the weight and complexity of the systems. The weight of all components on any aerospace system is highly important, as this greatly affects both price and performance. Current methods of protecting circuit boards from vibration and their associated stresses significantly add to the weight of aerospace electronic systems. This includes bulky mounting fixtures, reinforcing ribs, and passive vibration damping mounts. Entire electronic subassemblies containing many ECBs may also be mounted together with vibration isolators protecting the circuit boards from the surrounding vibrations. These reinforced ECBs and vibration isolation systems consume considerable space and add significant weight to these aerospace electronic systems. The vibration protection they provide is crucial, however, as the vibration environment of aerospace vehicles requires an extremely robust, durable mechanical design to prevent premature failures. By directly mounting an active mass damping system onto each ECB, it is possible to reduce significantly the weight and volume of the entire ECB system while maintaining equal or superior vibration protection.

*Corresponding author. Tel.: +1-802-656-1933; fax: +1-802-656-1929.
E-mail address: besser@emba.uvm.edu (B. Esser).

0022-460X/$ - see front matter
doi:10.1016/j.jsv.2003.11.055

The benefits of this technology could be most important in space applications, since weight is so closely related to cost and performance. Current transportation costs to geosynchronous orbits using a NASA reusable launch vehicle are close to $US 10 000 per pound of payload [2]. Savings of even a few pounds can add up to millions of dollars over the service life of an aircraft. Using integrated active damping systems on each ECB could reduce the total weight of an electrical system by up to 10–15%. Also, the space required to house and mount the electronics would be significantly reduced. Successful implementation of an integrated active damping system on the electronic systems could denote a significant breakthrough in terms of both affordable access (cheaper, smaller space vehicles) and the ability to launch higher performance systems in smaller packages. Also, spacecraft of lighter weight have more options regarding orbits and trajectories, as their reduced inertia will cause less influence from gravitation and better response from onboard propulsion systems. These new, lightweight satellites and spacecraft will become the "sportscars" of space. Reducing the cost of payload delivery to orbit will increase the availability and promote the commercial use of geosynchronous orbit. Weight savings on manned space vehicles may allow for additional crew or the incorporation of other desired systems which were previously beyond the weight limits of the vehicle. The National Security Space Roadmap (NSSRM) cites the need for "advanced integrated structures" which "improve payload mass-fraction, reduce satellite assembly time, and reduce overall costs". In addition, the NSSRM has the objective to "reduce launch vehicle costs and weights by at least 50% and cut lead times by a third through the application of advanced composite materials and structural designs". Also, applying this technology to both commercial and military aerospace applications will result in similar benefits: lower cost and higher performance.

There are several types of active vibration control systems that have been used successfully in various applications. These include active base isolation systems, structural actuators, variable damping and stiffening elements, and active mass dampers. Due to the geometric peculiarities of ECBs and other packaging considerations, including the desire for a minimal redesign of the ECB, active mass dampers are an attractive system for this application.

The operating principle of an active mass damper is that it counteracts the vibrations of an object by driving a small mass in an out of phase motion. The inertia forces of the mass quell the vibrations. The primary effect of active mass damping systems is to modify the level of damping in

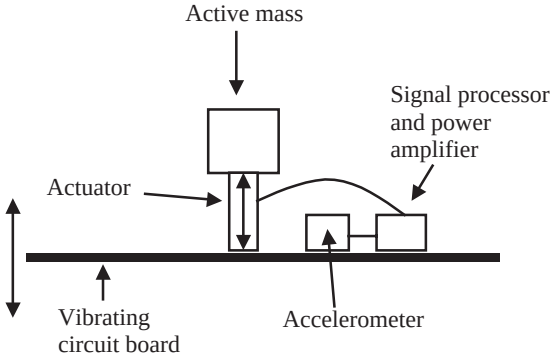

Fig. 1. Main components of an active mass damper system.

a structure with only minor modifications of stiffness. The main components of the system are shown in Fig. 1. These are: (1) Active mass—this is a mass that is attached to the vibrating structure. The mass of this active component usually ranges from 1% to 10% of the mass of the vibrating structure. (2) Actuator—this is an electromechanical device that drives the active mass out of phase with the vibrations. The actuator will most likely be either a voice coil electromagnetic device, or a piezoelectric device. (3) Transducer—this will sense the vibrations of the structure. It will most likely be a MEMS-based accelerometer. (4) Signal processor—the vibrations measured by the transducer will be processed to produce a control signal for the actuator and the inertial mass. The signal processor can be either an analog-based system using operational amplifiers, or a combination of analog and digital signals using a microprocessor to control the active mass. (5) Power amplifier—the control signals generated by the signal processor will be amplified to power amplifier to drive the inertial mass.

2. Theory

The mechanics associated with mass damping, both tuned mass damper (TMD) and active mass damper (AMD), are described in this section. TMDs are typically single-degree-of-freedom add-on devices which can work in one of two ways. They may serve to shift the natural frequency of the combined system to a more desirable (less excited) frequency, or they may simply absorb energy from the system through traditional damping. The first operation principle is useful when vibration excitation sources are of one known frequency, but are limited in applications of broadband or non-periodic excitation. The mass of a TMD is usually between 0.1% and 20% of the mass of the object requiring damping. Very small mass ratios, however, are very sensitive to becoming detuned due to a variety of slight changes in a system, so ratios over 0.5% are recommended.

Fig. 2 illustrates a system undergoing base excitation in the z direction. The circuit board, designated m_b, has an associated stiffness k_b and damping coefficient c_b. The mass damper, m_d, applies a force to the board, F_d. The absolute displacements of the board and damper are given by x_b and x_d, respectively. The relative motions of the board and mass damper to the base are given by y_b and y_d, respectively. Applying Newton's second law to each of the masses yields two equations of motion. For the board

$$m_b\ddot{x}_b = F_d - k_b y_b - c_b\dot{y}_b \tag{1}$$

and for the damper

$$m_d\ddot{x}_d = -F_d. \tag{2}$$

The equations for the relative displacements and accelerations of the board and damper, measurable quantities, are given by

$$x_b = y_b + z, \qquad x_d = y_d + z, \qquad \ddot{x}_b = \ddot{y}_b + \ddot{z}, \qquad \ddot{x}_d = \ddot{y}_d + \ddot{z}. \tag{3}$$

Combining the equations yields

$$m_b\ddot{y}_b + c_b\dot{y}_b + k_b y_b = F_d - m_b\ddot{z}, \qquad m_d\ddot{y}_d = -F_d - m_d\ddot{z}. \tag{4, 5}$$

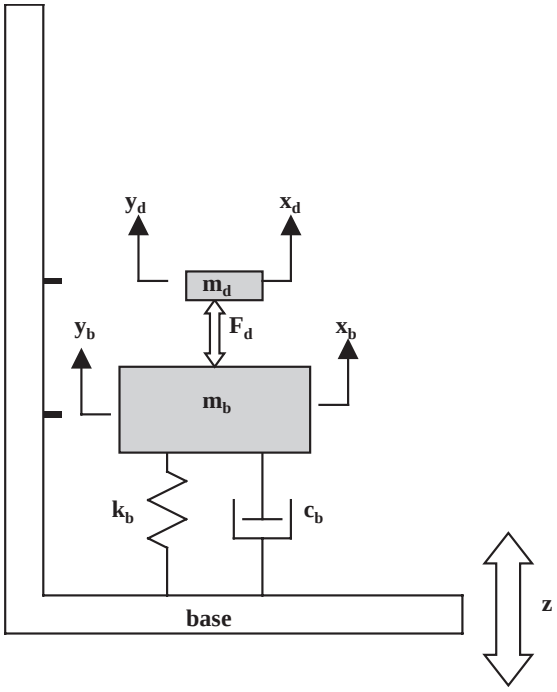

Fig. 2. Diagram of a mass damping system.

These describe the system for various cases. For a passive TMD, the damping force is given by

$$F_d = k_d(y_d - y_b) + c_d(\dot{y}_d - \dot{y}_b) \tag{6}$$

which yields

$$m_b\ddot{y}_b + (c_b + c_d)\dot{y}_b - c_d\dot{y}_d + (k_b + k_d)y_b - k_d y_d = -m_b\ddot{z}, \tag{7}$$

$$m_d\ddot{y}_d - c_d\dot{y}_b + c_d\dot{y}_d - k_d y_b + k_d y_d = -m_d\ddot{z}. \tag{8}$$

Optimizing these two relationships and simplifying yields the Den Hartog criterion for determining the ideal damper to structure frequency ratio, shown in Eq. (9) below. This relationship is based on minimizing the maximum of the frequency response function. Damping of the primary mass is assumed to be zero, which is the case for "frequency shifting" TMDs, which rather than actually providing damping, serve to shift the natural frequency of the combined system away from the problematic excitation frequency. This method was first proposed by Ormondroyd and Hartog in 1928 [3].

$$\frac{f_d}{f_s} = \frac{1}{1+\mu}. \tag{9}$$

Here, f_d is the freestanding natural frequency of the damper, f_s is the frequency of the undamped structure, and μ is the ratio of the TMD mass to the structure mass.

For the case of a system undergoing steady state sinusoidal excitations and having acceleration feedback to an active damping element, the following equations govern the motions of the base,

board, and damper:

$$z(t) = Z\mathrm{e}^{\mathrm{i}\omega t}, \qquad y_b(t) = Y_b\mathrm{e}^{\mathrm{i}\omega t}, \qquad y_d(t) = Y_d\mathrm{e}^{\mathrm{i}\omega t}, \tag{10}$$

$$\ddot{z}(t) = -\omega^2 Z\mathrm{e}^{\mathrm{i}\omega t}, \qquad \ddot{y}_b(t) = -\omega^2 Y_b\mathrm{e}^{\mathrm{i}\omega t}, \qquad \ddot{y}_d(t) = -\omega^2 Y_d\mathrm{e}^{\mathrm{i}\omega t}$$

which are used to derive the expression for the acceleration of the board in terms of its relative displacement and the motion of the base:

$$\ddot{x}_b(t) = \ddot{y}_b(t) + \ddot{z}(t) = -\omega^2(Y_b + Z)\mathrm{e}^{\mathrm{i}\omega t}. \tag{11}$$

Utilizing acceleration-based feedback and implementing a complex gain function, G, having both magnitude and phase components, describes the force supplied by the damper in terms of

$$F_d(t) = G\mathrm{e}^{\mathrm{i}\phi}\ddot{x}_b(t) = -\omega^2 G\mathrm{e}^{\mathrm{i}\phi}(Y_b + Z)\mathrm{e}^{\mathrm{i}\omega t}. \tag{12}$$

Inserting this expression into equations of motion (4) and (5) for the board and damper, and solving for the displacement of the board, Y_b, gives

$$Y_b = \frac{(m_b - G\mathrm{e}^{\mathrm{i}\phi})\omega^2 Z}{[(k_b - m_b\omega^2) + \mathrm{i}c_b\omega + G\mathrm{e}^{\mathrm{i}\phi}\omega^2]}. \tag{13}$$

From this it can be seen that if $|G| = -m_b$, then $Y_b = 0$, i.e., the relative motion or flexure of the board is zero. However there are real-world limitations of F_d, such as the stroke of the actuator. There are numerous ways to constrain the system so as to account for the real-world limitations. One such method is to limit the ratio of the gain to the board mass, G/m_b. Multiplying the numerator and denominator of Eq. (13) by $1/(m_b\omega_b^2)$, and substituting $\zeta = c_b/(2m_b\omega_b)$ as the damping ratio, Eq. (13) can be written as

$$Y_b = \frac{(1 - G\mathrm{e}^{\mathrm{i}\phi}/m_b)\Omega^2 Z}{[(1 - \Omega^2) + 2\mathrm{i}\zeta\Omega + G\mathrm{e}^{\mathrm{i}\phi}\Omega^2/m_b]}, \tag{14}$$

where Ω represents the normalized ratio of excitation frequency, ω, to the board's natural frequency, ω_b. Deflections predicted by this model will be compared to the experimentally collected results.

One key aspect of this relationship is developing the gain function to maximize the performance of the system for a range of excitation frequencies and amplitudes, resulting in a robust control system for the active mass damper. It can be seen that, where a TMD can reduce the amplitude of vibration through shifting the phase or energy dissipation through damping, an active system has the potential to actually cancel out the inertial forces acting on the ECB, resulting in much better performance over a range of operating parameters.

3. Experimental apparatus

Initial experiments were carried out on a simple laboratory testbed, shown in Fig. 3. This system consists of a rigid board suspended from an inertial base through the use of soft elastic springs. A circuit board is mounted to the top side of this plate with standoffs, and a Wilcoxon inertial shaker, model F4/Z820WA, is mounted to the bottom side. A small inverted voice coil

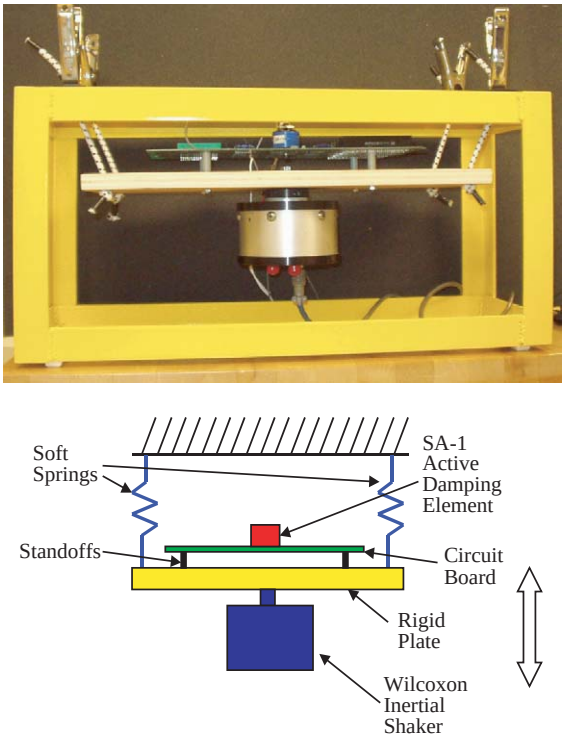

Fig. 3. Experimental vibration testbed.

actuator (CSA model SA-1) was mounted to the center of the board to act as the active mass damper (traditional voice coils move a coil inside a permanent magnet, but for better performance, i.e., higher active mass to total mass ratio, moving the magnets within the coil is preferred).

The apparatus consists of three independent electrical systems: the shaker system, the active damping system, and the measurement system. The shaker system includes a function generator providing a sinusoidal output, which is then amplified and sent to the inertial shaker. The active mass control system uses data from a MEMS-based accelerometer (Analog Devices ADXL150) mounted to the ECB, shifts the phase using an analog variable phase shifter circuit, then amplifies the signal to control the motions of the active mass damper. The phase shift circuit is a series of simple unity gain op amps with potentiometers that are tuned to provide specific phase delays. A quarter bridge strain gage circuit mounted directly to the board adjacent to the active mass component provided a measure of the flexural strain in the board and overall system performance.

With this simple setup, data were collected to determine the ability of the system to damp the fundamental vibration mode of the ECB as mounted. LabView software running on a PC provided a data acquisition interface. MatLab software was utilized to perform the data analysis and graphing. Fig. 4 shows a diagram of the complete system.

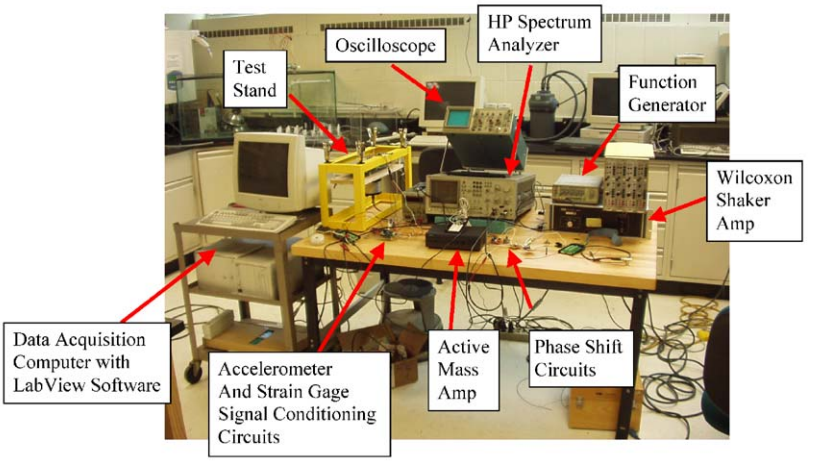

Fig. 4. Complete vibration analysis system.

4. Results and discussion

Initial evaluations of the board were designed to determine the natural frequency and measure the board's response as mounted to a range of frequencies. It was found that at the first resonant frequency, 50 Hz, the deflection magnitude of the board, and the resulting strain levels, were an order of magnitude higher compared to frequencies slightly above and below resonance. As the goal of this project is to demonstrate that active mass damping can increase the durability and longevity of the circuit board while reducing weight, it was taken as the goal to minimize the board strain at this fundamental mode, which is presumably also the mode most damaging to the integrity of the board.

As a check of stability, the experimental model, Eq. (4), was evaluated for stability for the case where the base excitation is zero. This was done using the non-dimensional form given by

$$\Omega = \frac{-i\zeta \pm \sqrt{-\zeta^2 - (Ge^{i\phi}/m_b) + 1}}{(Ge^{i\phi}/m_b) - 1}. \tag{15}$$

For a damping ratio of 0.02, the stability of the system as determined from the roots of the characteristic equation corresponding to the homogeneous solution to the governing differential equation can be seen in Fig. 5. This solution shows that to ensure stability, the gain ratio of the feedback circuit, G/m_b, must be kept low enough to prevent the system from going unstable across all phase delays. Using this criterion, the performance of the AMD in reducing board strain was evaluated.

In order to determine the ideal signal phase shift from the board mounted accelerometer to the active mass device, an experiment was conducted in which the phase shift was varied while holding the gain of the AMD constant and observing the response of the system. Fig. 6 shows these results.

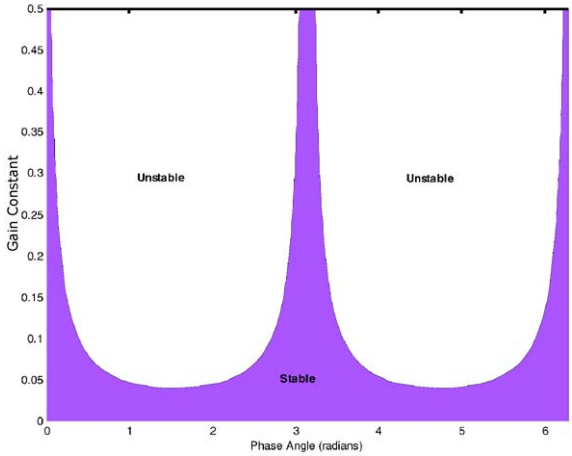

Fig. 5. Model stability (damping = 0.02).

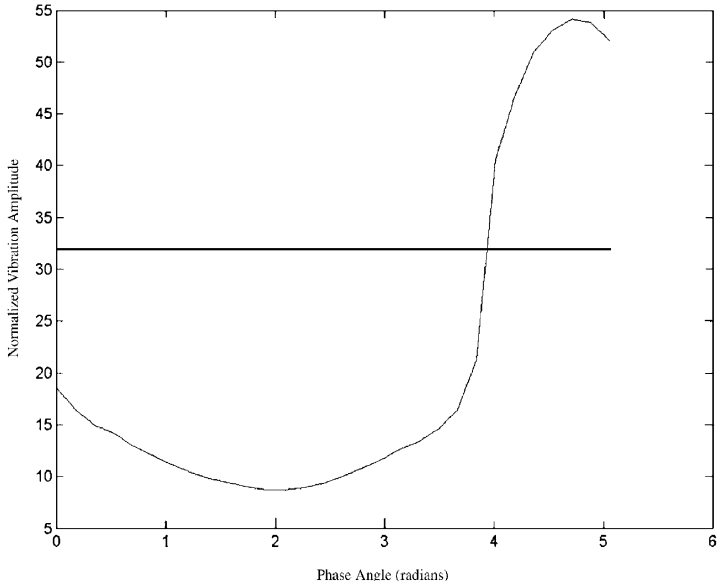

Fig. 6. Experimental vibration amplitude versus AMD phase shift.

It can be seen that at a phase shift of 110–120° the r.m.s. amplitude of vibration is reduced by 73%. Other experiments at various frequencies both above and below resonance were carried out. However, the reduced board strains at these levels reduced the effectiveness of the AMD. Above resonance, at 60 Hz, the maximum reduction was 11% at a signal phase shift of 50°. At 40 Hz strains were reduced by 56% at a phase shift of 140°.

Fig. 6 shows that at a phase shift of about 115°, the system does a very good job of reducing the strain in the board undergoing harmonic excitation. Eq. (14) predicts a similar response of the system under these conditions. For a damping ratio of 0.02 and a G/m ratio of 0.02, the

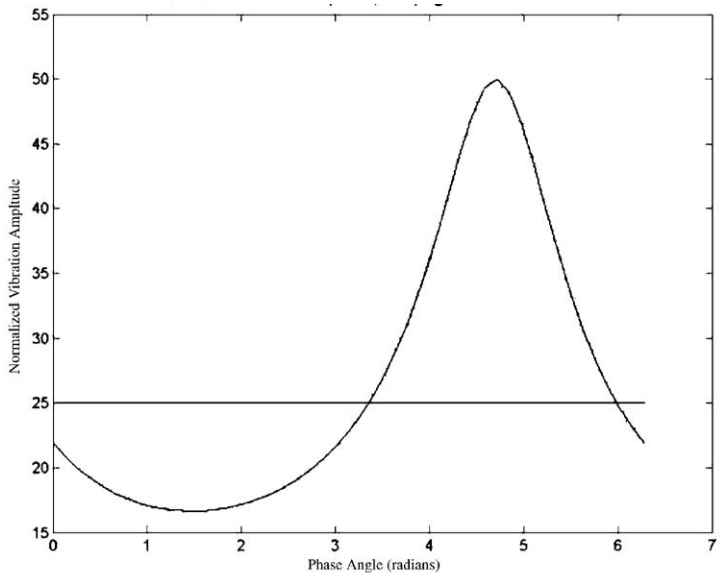

Fig. 7. Predicted vibration amplitude versus AMD phase shift (damping = 0.02, AMD gain = 0.02).

normalized magnitude of the deflection of the board over a range of signal phase shifts is shown in Fig. 7, as is the zero gain case. This prediction, however, is based on the mechanical phase delay between the actuator and the motion of the board, whereas Fig. 6 displays the response of the board as a function of the signal phase delay.

Similar experiments above and below resonance reveal that below resonance the system can be tuned to reduce board strains by about 56%, while above resonance only minimal reductions were achieved. However, since these excitation frequencies produce much smaller board strains, a simple active mass damping system can be tuned to quell vibrations at or near resonance using an appropriate low-pass filter.

6. Conclusions

Future work on this project will include implementing a low-pass filter and observing the response of the system to random noise input, while tuning the AMD to damp out the fundamental 50 Hz mode. Provided this is successful in significantly reducing the strain levels in the board, a stand-alone analog AMD system can be easily packaged for implementation on a circuit board for aerospace applications. Constructing a robust unit which has a variable low-pass cutoff for a variety of circuit board natural frequencies is possible. There are many other avenues of future work to explore. These include: a complete vibration analysis of the system, including higher order modes, using specialized vibration analysis software and equipment; development of optimal control strategies to provide robust damping characteristics over a range of excitation frequencies and amplitudes; a comparison with state of the art ECB damping techniques, both in

terms of damping characteristics and overall system weight; design of an integrated MEMS-based system; and a detailed cost analysis, both in terms of implementation costs and savings potentials.

By producing self-contained AMD modules that are located on and powered by the ECB's existing infrastructure, lighter ECBs can be produced. Also, the mounting methods and vibration isolation components of the ECB housings can be simplified and the weight significantly reduced.

The vision for this system is to have these AMD modules integrated into the manufacture of the ECB from the start, as opposed to an after the fact add on. By locating the ideal placement of the AMD modules, determined through the use of specialized software, the ECBs can be made much thinner and lighter, and would essentially take care of themselves once installed in, and powered by, an aerospace platform. The potential benefits of widespread use of these AMD modules are numerous. They include better fuel efficiency, longer range, higher launch altitudes, reduced system complexity, larger payload capacities, and increased durability.

As the AMD modules come down in price and are produced in numerous configurations, uses will expand to include many applications. These include, but are not limited to, land vehicles, commercial applications, machinery installations, and basically anywhere vibration may cause failure of an electronic circuit board.

Acknowledgements

This work was supported by NSF VT-EPSCoR. Use of the SA-1 actuator was provided by Sean Fahey and Michael Evert of CSA Engineering, Mountain View, CA.

References

[1] D.S. Steinberg, *Vibration Analysis for Electronic Equipment*, 2nd Edition, Wiley, New York, 1988.
[2] I.A. Curtis, M.K. VanDyke, Affordable in-space transportation, NASA Technical Memorandum 108521, Marshall Space Flight Center, October 1996.
[3] J.P.D. Hartog, *Mechanical Vibrations*, 4th Edition, McGraw-Hill, New York, 1956.